

Selection of Optimal Process Analyzers for Plant-Wide Monitoring

Frans W. J. van den Berg,^{†,‡} Huub C. J. Hoefsloot,[§] and Age K. Smilde^{*,†}

Process Analysis and Chemometrics, Department of Chemical Engineering, University of Amsterdam, Nieuwe Achtergracht 166, 1018 WV Amsterdam, The Netherlands

In this paper, the effect of process analyzer selection and positioning on plant-wide process monitoring is investigated. A fundamental problem in process analytical chemistry is the incomparability of different instrument characteristics. A fast but imprecise instrument is incomparable to a slow but precise instrument. Theory is developed to overcome this problem by using an abstract definition of a process analyzer. This definition allows us to put all instrument characteristics for a particular monitoring task on an equal footing. This results in a measurability factor M that expresses monitoring performance of any process measurement by combining instrument characteristics such as precision, sampling rate, grab size, response correlation, and delay time. Both the choice of location and the performance characteristics of different process analyzers can be evaluated using the measurability factor. The unifying nature of the measurability factor allows for a rational decision between completely different process analyzers and locations (Smilde et al., in this issue). The theory is illustrated and validated with an experiment. A tubular reactor for free-radical bulk polymerization of styrene is monitored by in-line short-wave near-infrared spectroscopy at different positions. Alternatively, product samples are collected for at-line near-infrared analysis. Both analyzers measure styrene monomer concentration. The analysis results are used to predict conversion as well as number and weight average molecular mass of the polystyrene reactor product. The theoretical measurability factors for this case study correspond well with the experimental findings.

An ever-increasing number of process analyzers are implemented in the chemical industry. At the same time, the diversity in techniques suitable for harsh process conditions—e.g., chromatography, (near)-infrared, and Raman or (low-field) nuclear magnetic resonance spectroscopy, mass spectrometry, flow injection analysis, and ultrasonic analysis, to name just a few—grows steadily.¹ The implementation and operation of analytical in-process measurements is, however, still relatively expensive. (The

expression “in-process” is an idiom for all at-line, on-line, in-line, and noninvasive measurement techniques suited for “real-time” monitoring or control of a process.) The cost of purchase and maintenance often limits the number of analyzers and process sampling interfaces that can be implemented for monitoring or control purposes to one or a few key components. This naturally leads to the following questions: what is the added value of process analyzers as compared to more conventional, inferential measuring devices such as temperature, pressure, or flow sensors; what is the better choice from the wide selection of process analyzers; and what is the best location to place this limited number of instruments? All these questions are related and can only be answered adequately by looking at the process under observation.^{2–7}

The “information content” of measured process variables is a function of the underlying process dynamics, the external process disturbances, and the process analyzer measuring these variables. The dynamic behavior of various important process variables, e.g., reactant versus product, can be quite distinct. An important objective is thus to sample the process variable with the most information in its measured signal, at the most informative position in the process (e.g., reactor inlet versus outlet). The characteristics of a process analyzer—e.g., slow but precise GC analysis versus fast but relative imprecise spectroscopic measurements—determine which technique is best suited for the analysis task at hand.

In our work, we distinguish the scientific or technological aspects (the so-called primary specifications) from the financial or organizational implications of a process analyzer implementation (the secondary specifications). We believe that the natural order of questioning is as follows: (1) what is the information gain achieved from a potential in-process analytical measurement; (2) does this gain justify the costs associated with instrument and process stream interfacing, the production downtime, training of

* To whom correspondence should be addressed. E-mail: asmilde@science.uva.nl.

[†] Process Analysis and Chemometrics.

[‡] Current address: Chemometrics Group, Food Technology, Department of Dairy and Food Science, The Royal Veterinary and Agricultural University, Copenhagen, Denmark.

[§] Department of Chemical Engineering.

- (1) Workman, J.; Veltkamp, D.; Doherty, S.; Anderson, B.; Creasy, K.; Koch, M.; Tatera, J.; Robinson, A.; Bond, L.; Burgess, L.; Bokerman, G.; Ullman, A.; Darsey, G.; Mozayeri, F.; Bamberger, J.; Stautberg-Greenwood, M. *Anal. Chem.* **1999**, *71*, 121R–180R.
- (2) Smilde, A. K.; van den Berg, F. W. J.; Hoefsloot, H. C. J. *Anal. Chem.*, A-pages in this issue.
- (3) van den Berg, F. W. J.; Hoefsloot, H. C. J.; Boelens, H. F. M.; Smilde, A. K. *AIChE J.* **2001**, *47*, 2503–2514.
- (4) van den Berg, F. W. J.; Hoefsloot, H. C. J.; Boelens, H. F. M.; Smilde, A. K. *Chem. Eng. Sci.* **2000**, *55*, 827–837.
- (5) van der Grinten, P. M. E. M. *Stat. Neerlandica* **1968**, *22*, 43–63.
- (6) Didden, C.; Duisings, J. *Process Control Qual.* **1992**, *3*, 263–271.
- (7) Harris, Th. J.; MacGregor, J. F.; Wright, J. D. *AIChE J.* **1980**, *26*, 910–916.

operators, etc., in relation to, for example, an improved controller performance or enhanced safety. In this paper, we will focus on the primary instrument specifications.

To assess the performance of process analyzers we identify six characteristics, the so-called *process analyzer dynamics*.³ The first characteristic is the process variable selected for measurement and the location at which it is sampled. The second contribution is instrument precision, the uncertainty or error encountered in every measurement. The third contribution is the sampling rate, the effect of making discrete measurements on a continuous process. The fourth contribution is “grab-size” error, the information loss introduced by collecting a sample of sufficient size. The fifth contribution is response correlation. This phenomenon is often observed in “physical” measurements such as ion-selective electrodes, pH, or conductivity, where instrument responses are correlated over time (a “memory” effect of preceding measurement responses). The sixth contribution is analysis or delay time, the time passed between collecting the sample and getting the analysis result. Obvious examples are separation-based composition analyzers that require some time to handle a sample before the result becomes available. These six characteristics must be taken into account when the performance of different in-process implementations is being assessed. Additional characteristics could be considered, but these six are sufficient to model most present-day process analyzers.

In this paper, we make use of a so-called Kalman state vector observer to estimate process variables from in-process measurements. The process state vector is a collection of all the important process variables such as concentrations of the different components or moments of the polymer product mass distribution. The process state vector's time trajectory thus shows the behavior of the process in time by showing the trajectory of all important process variables in it. Many of the process state vector elements, e.g., the mass distribution, cannot be measured directly. The input to the Kalman state observer is the measurement result from the process analyzer, measuring, for example, the monomer concentration. The output of the state observer is an estimate of the complete state vector. It contains both filtered results of the measured process variables (the monomer concentration) and estimated values for the unmeasured process variables (the mass distribution). To make an estimate of unmeasured process variables, the state observer uses a fundamental process model based on, for example, mass balances of the different reacting species.

The Kalman observer also provides an expected estimation error in the form of a theoretical covariance uncertainty matrix of the estimated state vector. The optimal analyzer type and location for a process is selected by minimizing this state vector estimation error. More details on the Kalman state observer can be found in the Appendix. To quantify the performance of a process analyzer implementation and state vector observer, we define the measurability factor M , ranging from 0 to 1, where one indicates perfect process state vector reconstruction. Perfect reconstruction in this context means that the process variables in the estimated state vector coincide with the true process variables for every point in time.

The theory on process analyzer selection and positioning is tested on experiments with a bench-scale continuous tubular

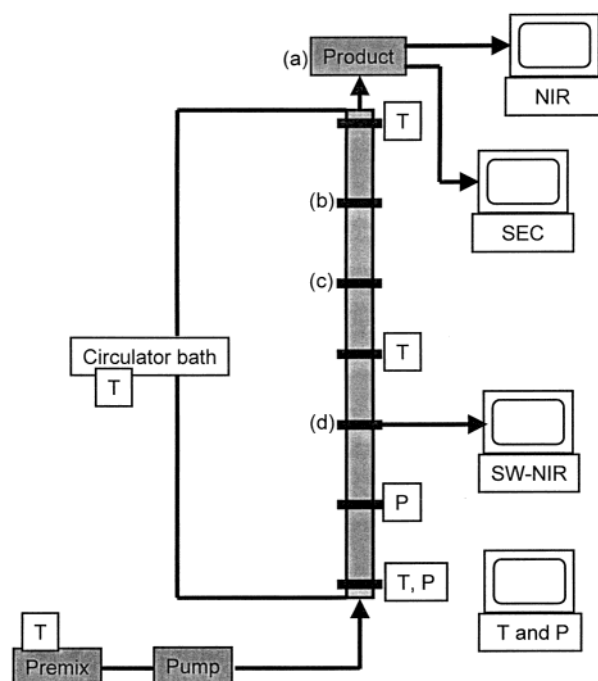


Figure 1. Overview of the bench-scale polystyrene tubular reactor setup. The characters a–d mark different process analyzer locations used in the Experimental Section.

reactor for free-radical bulk polymerization of styrene to polystyrene.^{8,9} At different locations along the reactor tube, in-line short-wave near-infrared (SW-NIR) spectroscopic styrene concentration measurements can be performed. At the same time, samples are collected at the reactor outlet for at-line near-infrared (NIR) spectroscopic styrene concentration analysis. In combination with a Kalman state observer, the different spectroscopic measurements can be used to predict molar mass distribution of the polystyrene product (M_n and M_w) at the reactor exit. The molar mass average predictions will be verified by off-line size exclusion chromatography (SEC).

THEORY

The theory will be explained using the styrene polymerization case study as a leading example. A schematic drawing of the tubular polymerization reactor is shown in Figure 1. Two types of spectroscopic in-process analyzers are available: in-line SW-NIR at one of seven locations along the reactor tube and at-line NIR on product samples. Styrene concentration is the measured process variable for both techniques. From this measurement, the process state vector containing all relevant process variables—initiator concentration $C_i(t)$, monomer concentration $C_m(t)$, and molecular mass distribution moments $M_n(t)$ and $M_w(t)$ —is determined by a state vector observer. Details of the measurement scheme are illustrated in Figure 2. Process variable $C_m(t)$ is measured in-line somewhere along the reactor tube or at-line on product samples. At every sample location, the $C_m(t)$ signal shows a distinct dynamic behavior (symbolized by T_m) and variance/amplitude (σ_m^2) as a function of the process dynamics and the

(8) Young, R. J.; Lovell, P. A. *Introduction to Polymers*; Chapman & Hall: London, 1991.

(9) Dotson, N. A.; Galvan, R.; Laurence, R. L.; Tirrell, M. *Polymerization Process Modeling*; VCH Publishers: New York, 1996.

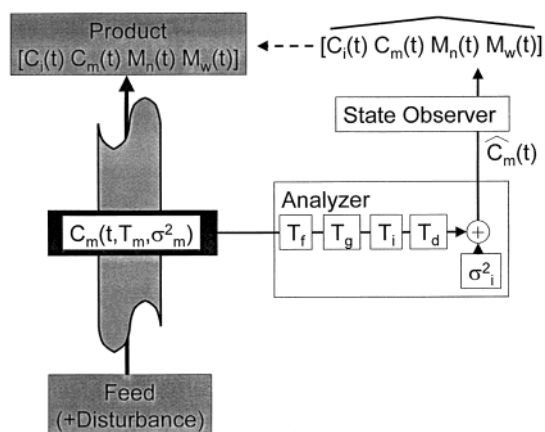


Figure 2. A detailed look at monitoring with a process analyzer.

external process disturbances. The analyzer with its distinct analyzer characteristics “processes” the sampled variable $C_m(t)$ and gives an estimated $\hat{C}_m(t)$ as measurement outcome. This analysis result is then fed to a process state observer that has the following task: invert the undesired signal processing by the analyzer and estimate the state vector (containing both measured and unmeasured process variables) for the reactor system.

To find the optimal in-process measurement configuration, we take six different aspects into consideration, loosely called the *process analyzer dynamics*.³ The first aspect is the process variable selected for measurement and the location at which this process variable is sampled. This selection is guided by the amount of information a variable contains on the overall dynamics of the process and the availability of a suitable in-process instrument for monitoring in “real-time” this variable at that particular location. Process engineers and analytical chemists should make a first selection of potential candidate analyzers and locations for a specific monitoring task. The methods we propose can then make a rational selection from this set. In our case study, the choice is limited to in-line SW-NIR or at-line NIR, measuring monomer concentration $C_m(t)$. Alternative measurement schemes could be developed for spectroscopic initiator measurements or on-line SEC. However, the low initiator concentrations in free-radical polymerization and the relative long analysis times required for SEC, a requirement incompatible with the relative fast dynamics in our reactor system, immediately classify them as unattractive alternatives for this system.

The second contribution of instrument characteristic is process analyzer precision σ_i^2 . Uncertainty in the instrument outcome will be approximated by the true concentration $C(t)$ plus additive white noise $v(t)$ with known distribution, typically determined during the calibration procedure or supplied by an instrument vendor.

$$\hat{C}(t) = C(t) + v(t) \quad v(t) = N(0, \sigma_i^2) \quad (1)$$

The third source of error is the sampling rate of the instrument, specified by the time interval between successive samples T_i (where the sample frequency is $1/T_i$). In-process analyzers typically make discrete observations on continuous processes. The state of the process—altered by external disturbances—can only be determined when a new analysis result comes in. Hence, the uncertainty can only be reduced when a new measurement

becomes available and a new state vector estimate is performed. For many instruments (e.g., spectrophotometers), there is a tradeoff possible between the sampling frequency $1/T_i$ and precision σ_i^2 . Spending more time per analysis to increase the signal-to-noise ratio will automatically lead to a lower sampling rate (further details are given in the Appendix).

The fourth analyzer characteristic is grab size T_g . If a sample is collected over a short period of time, for example, to gather enough material for physical experiments or to get sufficient detector signal for spectroscopy, the expected value of the measurement will be the average value over that same time period. Hence, variability during that period goes undetected. This average value becomes available once the entire grab has passed. If this grab size is relatively short, we can associate the analysis result with the true value at time equal to half the grab time interval. Therefore, in our *process analyzer dynamics* we penalize grab size with a time delay of half the grab time T_g .

$$\hat{C}(t) = C(t - 0.5T_g) + v(t - 0.5T_g) \quad (2)$$

In words, eq 2 would read: the estimate of process variable C we retrieve at time t is really an estimate of this variable $0.5T_g$ time units ago. As a consequence, information on the continuously changing C signal is already $0.5T_g$ time units “old” before we get it. The same reasoning holds for precision $v(t)$.

The fifth contribution to process analyzer performance is response correlation T_i . In many instruments, there is significant carry-over in the detector response from one measurement to the next (e.g., pH ion-selective electrodes or temperature-dependent resistors). This carry-over can be approximated by an exponentially first-order correlation of the autoregressive form.

$$\hat{C}(t) = (1 - e^{-1/T_i})C(t) + e^{-1/T_i}C(t - T_i) + v(t) \quad (3)$$

The noise $v(t)$ is scaled to have equal magnitude as the uncertainty in eq 1. The final estimate is written as an exponentially weighted sum of present and previous values of the sampled variables, where the weights are determined by the response correlation time constant T_i between successive measurements. When T_i is very small, say zero, then the term containing T_i vanishes and the effect of the correlation time is canceled.

The last component describing the performance of in-process instrumentation is the analysis or delay time T_d between taking the sample and obtaining the analysis result.

$$\hat{C}(t) = C(t - T_d) + v(t - T_d) \quad (4)$$

In words, information on the continuously changing C signal is already T_d time units “old” before we get it. An example of an analyzer with a significant time delay is in-process chromatography, where the components first have to be physically separated before the final analysis results become available.

The six contributions to *process analyzer dynamics*—the process variable and location selected for measurement plus the five instrument characteristics—as formulated above give us a more abstract definition of in-process analyzers. It enables us to compare completely different measurement techniques—e.g., GC versus

NIR spectroscopy—on a theoretical level, comparing their individual merits on conceptual grounds. The goal of all analyzer/observer combinations is the same: to estimate the process state vector, which holds the process variables considered important. Optimal selection of instrument type and location must guarantee that sufficient information is obtained from a measurement to make a good “real-time” estimate of the state vector.

In this paper, we use the Kalman observer to estimate the process state. This observer is an unbiased, minimum variance, and consistent estimator for the process state of a linearized system.^{10–12} Further details on reactor dynamics and the observer are given in the Appendix.

To assess the performance of different process analyzers, we have developed the measurability factor M .^{3,5} For a stable process such as the tubular polymerization reactor in our case study, M will be a scalar between 0 and 1, where one indicates perfect process state vector estimation. A stable process perturbed from normal operation conditions by external process disturbances—e.g., variations in initiator concentration of the feed stream in our example—will operate within a limited range surrounding these normal operating conditions. We can express this variation in the form of a process covariance matrix \mathbf{Q} . In our reactor tube, \mathbf{Q} thus gives the range or boundaries of the composition of the reactor product stream over time due to expected disturbances in the reactor feed. The task of the process analyzer and observer is to estimate the exact position of the process state vector—with all the important process variables—within this operating range surrounding the normal trajectory. Moreover, this estimate should be available for every point in time. Because of the *process analyzer dynamics*, this state estimate will, however, never be perfect. We can express the estimation error or uncertainty due to analyzer characteristics in the form of a covariance matrix \mathbf{P} . From the covariance matrices \mathbf{Q} and \mathbf{P} we can compute the measurability factor M .

$$M = \frac{\text{trace}(\mathbf{Q}) - \text{trace}(\mathbf{P})}{\text{trace}(\mathbf{Q})} \quad (6)$$

The “trace” is the sum of diagonal elements of the covariance matrices and serves as a norm for the matrix involved. In our case study, this is equal to summing (expected) variances for all the relevant process variables in the reactor state vector. $\text{trace}(\mathbf{Q})$ is the unknown process variance caused by external process disturbances, and $\text{trace}(\mathbf{P})$ is the prediction error after measurement and state vector estimation. The numerator part of eq 5, $\text{trace}(\mathbf{Q}) - \text{trace}(\mathbf{P})$, is thus the removed unknown process variance. The measurability factor M in eq 5 thus approaches 1 when the $\text{trace}(\mathbf{P})$ approaches zero. For an extremely poor choice of a process analyzer, the covariance matrix \mathbf{P} after state vector estimation could be larger than the initial process uncertainty in \mathbf{Q} . In this (hypothetical) case, the measurability factor will get a negative value, which means that the in-process measurements serve no purpose, and our “best guess” for the process state vector

is the following: somewhere in the operating range surrounding the normal trajectory. The measurability factor in eq 5 thus shows how much of our initial uncertainty in knowledge of the process state vector is removed by the process analyzer and observer. The theory in this paper can easily be generalized to evaluating different combinations of multiple process analyzers for different estimation tasks.

EXPERIMENTAL SECTION

A bench-scale tubular reactor is constructed for the operation of a free-radical bulk polymerization of styrene in continuous mode. A drawing of the instrumentation is shown in Figure 1. The heart of the setup is a vertically placed stainless steel tube (1.1-m length; 10-mm i.d.) with seven gaugeable tube fitting union crosses. Teflon connectors can assemble different sensors in these crosses. Three thermocouples and two pressure sensors are inserted at different locations. Quartz windows for the in-line SW-NIR spectrometer are mounted in similar Teflon parts. By positioning windows on opposite sites in one cross piece, an in-line “cuvette” is created that can be sampled by the spectrometer (effective path length ± 8 mm).

The temperature inside the reactor tube is regulated by a circulator water bath and six cross-wise connected aluminum pipes placed along the inner reactor tube. The system is isolated to minimize heat loss. The temperature of the circulator bath is logged. A feed vessel and HPLC pump supply a continuous stream of styrene and AIBN initiator to the reactor entrance (flux, 2 mL·min⁻¹; average residence time, 42 min). The temperature of the premix is logged.

Product samples are collected from the reactor outlet in grabs of 3 min every 10 min. The styrene concentration is determined by at-line NIR spectroscopy. M_n and M_w for the polymer molar mass distribution in the product stream are determined off-line by SEC.¹³ Multivariate calibration was used for both spectroscopic techniques. The preprocessing and calibration results are shown in Table 1. Using the theory of *process analyzer dynamics*, the performance of the two instruments can be characterized as shown in Table 2.

The process disturbance is a $\pm 25\%$ uncertainty from the normal 0.04 mol·L⁻¹ initiator concentration of the reactor feed. The range of this process disturbance is used to compute the measurability factor M for different process analyzers and state observers. During the experiments, this disturbance was simulated by switching between three premix vessels with different (known) initiator concentrations.

RESULTS AND DISCUSSION

The objective of in-process measurements in our case study is to estimate the styrene conversion, and from that knowledge determine polystyrene molar mass distribution of the reactor polymer product. The best position for the in-line SW-NIR and the performance of the at-line NIR can be determined from the measurability factor M indicating the ability to estimate conversion. This factor can be computed using the dynamic reactor model and expected process disturbances as formulated in the Appendix, together with the process analyzer characteristics as specified in

(10) Jazwinski, A. H. *Stochastic Process and Filtering Theory*; Academic Press: San Diego, 1970.

(11) Gelb, A. *Applied Optimal Estimation*; The M.I.T. Press: Cambridge, MA, 1974.

(12) Grewal, M. S.; Andrews, A. P. *Kalman Filtering*; Prentice Hall: Englewood Cliffs, NJ, 1993.

(13) Lousberg, H. H. A.; Hamersma, P. J.; Iedema, P. D.; Ruitenber, E., submitted.

Table 1. Calibration NIR and SW-NIR Analysis

	NIR	visual/SW-NIR
integration	90 s (30 scans) 3499–10000 cm^{-1} 2 cm^{-1} (resolution)	15 s (± 150 scans) 400–1000 nm 1-nm interval (resolution)
Savitzky-Golay filter ¹⁴	37-points second derivative second-order polynomial	31-points fourth derivative fourth-order polynomial
spectral range used in PLS1	5618–6390 cm^{-1}	860–890 nm
PLS1 model ¹⁶ (partial least squares)	data mean centered 3 latent variables	data mean centered 4 latent variables
conversion uncertainty	0.2%(m/m) (RMSEP _{cv})	0.4%(m/m) (RMSEP _{cv})

Table 2. Process Analyzer Characteristics

	NIR	SW-NIR
σ_i	0.2%	0.4%
T_i	600s	35s
T_g	180s	15s
T_i	0s	0s
T_d	420s	20s

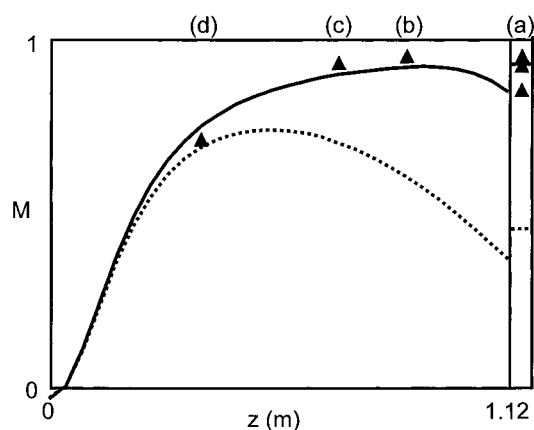


Figure 3. Theoretical measurability factor M as a function of in-line SW-NIR on position z in the reactor tube. Optimized for reactor product composition (—) or entire tube contents (···). The bar after $z = 1.12$ m gives the theoretical measurability factor for at-line NIR on reactor outlet samples. Triangles mark the *practical measurability factors* for three different experiments.

Table 2. The result is shown as the solid curve in Figure 3. From this figure, we observe that the better location for in-line SW-NIR analysis is in the second half of the reactor tube ($z \approx 0.6$ – 1.0 m). In-line SW-NIR measurements for the first part of the reactor tube ($z < 0.40$ m) are incapable of picking up process disturbances and estimating the reactor product composition, resulting in a low score for the measurability factor M in this segment. The slower but more precise at-line NIR measurement on product samples is slightly better than the optimal in-line SW-NIR implementation.

To verify our theoretical measurability, we have conducted three experiments for different SW-NIR positions: $z = 0.88$, 0.72 , and 0.40 m. In Figure 4, the estimated styrene conversion in collected product samples is plotted as a function of time. Also shown are reference values for product samples and the target value for normal operation conditions. The variance between the normal and the reference values represent the range of process variance in the product caused by the disturbances, in our case, initiator concentration changes in the feed stream. The difference between references and observer estimates quantify the residual

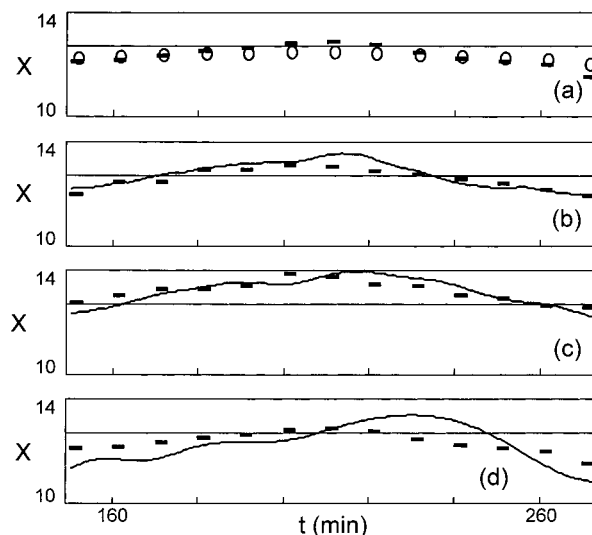


Figure 4. Estimated degree of styrene monomer conversion X (%) in reactor product. Bars are the reference values; horizontal line corresponds to normal operation. Predictions from (a) at-line NIR (O; results shown for one experiment) and in-line SW-NIR (—) on position (b) $z = 0.88$ m, (c) $z = 0.72$ m, and (d) $z = 0.40$ m.

uncertainty after making a reactor state vector estimate. From these two variances, a practical measurability factor, similar to the one given in eq 5, can be computed. It shows how well we can estimate styrene conversion in the reactor product using a particular measurement. The practical measurability factors are shown as triangles in Figure 3. Although there is some variation in the outcomes, as evident from the triplicates for at-line NIR analysis, the results for the theoretical and the practical measurability factors correspond well. The two computed moments of the polymer product molar mass distributions (M_n and M_w) are shown in Figure 5, together with the SEC reference values and normal values. Due to the “stiffness” of the styrene polymerization dynamics, the relative small changes in feed initiator concentration have only minor effects on the MMD.^{8,9,14}

EXTENSIONS

The optimization method of process analyzer selection and positioning presented in this paper can already be utilized in an early process design stage. From a dynamic process or unit operation model, an expected (range of) process disturbance(s) and process analyzer characteristics, the theoretical measurability

(14) Press, W. H.; Teukolsky, S. A.; Vetterling, W. T.; Flannery, B. P. *Numerical recipes in FORTRAN: the art of scientific computing*; Cambridge University Press: Cambridge, U.K., 1992.

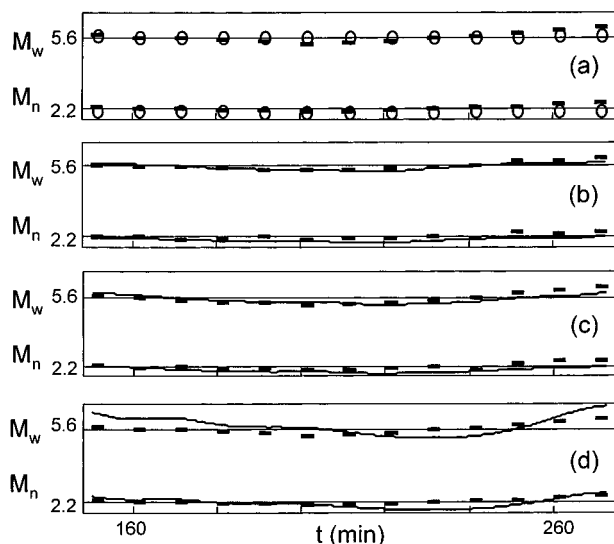


Figure 5. Estimated M_n and M_w ($\times 10^4$) for reactor polymer product. Bars are the reference values; horizontal line corresponds to normal operation. Predictions from (a) at-line NIR (\circ ; results shown for one experiment) and in-line SW-NIR (—) on position (b) $z = 0.88$ m, (c) $z = 0.72$ m, and (d) $z = 0.40$ m.

factors M can be computed without actually collecting any experimental data. To elucidate this point we refer back to the Theory section where it was stated that concentration of the monomer, as target for in-process analysis, is preferred over initiator concentration or molecular mass distribution moments. To reach an acceptable M value of, for example, 0.8 for our monitoring objective of estimating conversion at the reactor outlet, one needs either a very precise method for initiator concentration or an exceptionally fast (less than 20-min analysis time) technique for determining polymer mass distribution. Both requirements are difficult to fulfill. Hence, without investigating specific instruments, the required *process analyzer dynamics* tell us that monomer concentration is the best or most affordable candidate for monitoring in this process.

So far our objective was defined as to determine the conversion of the reactor product. To illustrate the versatility of the theory, we will briefly describe a different monitoring task. Suppose that the objective for this process analyzer and state vector observer combination is to estimate conversion for the entire reactor tube length. The purpose could, for example, be model predictive control, anticipating process regulation based on the (estimated) reactor state vector.¹⁵ The broken line in Figure 3 shows the measurability factor M for this analyzer/observer objective. The outcome illustrates that different monitoring objectives can lead to completely different results: the theoretical measurability factor is overall lower (the estimator task is more complex), the best location for in-line SW-NIR shifts toward the reactor inlet, and the at-line NIR is ineffective for this job.

CONCLUSIONS

In this paper, we have developed and applied the theory of optimal process analyzer selection and positioning on spectroscopic concentration measurements in a bench-scale tubular

reactor for free-radical bulk polymerization of styrene to polystyrene. The performance of different in-process instruments and state vector observers is evaluated as a function of the *process analyzer dynamics*. Both the choice of location and the performance characteristics of different instruments can be assessed using the measurability factor M . The theoretical performance for predicting product composition by both in-line SW-NIR and at-line NIR analysis is shown to correspond well with the experimental results. It is shown that in selecting an analyzer and sample position, the dynamics of the measured process variable and its information content regarding other (unmeasured) process variables is important. It is also shown to be a function of the dynamics of the instruments and the monitoring objective.

Through the measurability decision criterion, we hope to formulate a guideline to counteract the more or less ad hoc practice for present process analyzer selection and positioning. It is the task of the (process) analytical chemist (together with system and control engineers) to provide sensible input for this optimization procedure.

ACKNOWLEDGMENT

This work was financially supported by "Nederlandse Organisatie voor Wetenschappelijk Onderzoek" (NWO). Hans Boelens is acknowledged for his contribution to this research.

APPENDIX

In this study, we estimate the process state vector of a tubular reactor for the initiator driven, free-radical bulk polymerization of styrene^{8,9} using a Kalman state observer.^{10–12} To implement the observer, mass balances in the form of partial differential equations are required for initiator concentration C_i , styrene monomer C_m , and the first three moments for chain length distribution of growing (λ) and terminated polymer (μ). Equation A1 is a mathematical model of the tubular reactor in our case study (t is time; z is axial position in the reactor tube; v is the linear flow velocity).¹³

$$\frac{\partial C_i}{\partial t} = -v \frac{\partial C_i}{\partial z} - k_d C_i \quad (\text{A1a})$$

$$\frac{\partial C_m}{\partial t} = -v \frac{\partial C_m}{\partial z} - k_p C_m \lambda_0 \quad (\text{A1b})$$

$$\frac{\partial \lambda_0}{\partial t} = -v \frac{\partial \lambda_0}{\partial z} - k_t \lambda_0^2 + k_{sp} C_m^2 + 2fk_d C_i \quad (\text{A1c})$$

$$\frac{\partial \lambda_1}{\partial t} = -v \frac{\partial \lambda_1}{\partial z} - k_t \lambda_0 \lambda_1 + k_{sp} C_m^2 + 2fk_d C_i + k_p C_m \lambda_0 - k_{trm} C_m (\lambda_1 - \lambda_0) \quad (\text{A1d})$$

$$\frac{\partial \lambda_2}{\partial t} = -v \frac{\partial \lambda_2}{\partial z} - k_t \lambda_0 \lambda_2 + k_{sp} C_m^2 + 2fk_d C_i + k_p C_m (2\lambda_1 + \lambda_0) - k_{trm} C_m (\lambda_2 - \lambda_0) \quad (\text{A1e})$$

$$\frac{\partial \mu_0}{\partial t} = -v \frac{\partial \mu_0}{\partial z} + (1 - 0.5z) k_t \lambda_0^2 + k_{trm} C_m \lambda_0 \quad (\text{A1f})$$

$$\frac{\partial \mu_1}{\partial t} = -v \frac{\partial \mu_1}{\partial z} + k_t \lambda_0 \lambda_1 + k_{trm} C_m \lambda_1 \quad (\text{A1g})$$

$$\frac{\partial \mu_2}{\partial t} = -v \frac{\partial \mu_2}{\partial z} + k_t \lambda_0 \lambda_2 + k_t z \lambda_1^2 + k_{trm} C_m \lambda_2 \quad (\text{A1h})$$

(15) Morari, M.; Lee, J. H. *Comput. Chem. Eng.* **1999**, *23*, 667–682.

(16) Martens, H.; Næs, T. *Multivariate Calibration*; Wiley: New York, 1989.

From (A1), the number M_n and weight average molar masses M_w can be computed ($M_m = 104.15 \text{ g}\cdot\text{mol}^{-1}$).

$$M_n \approx M_m(\mu_1/\mu_0) \quad M_w \approx M_m(\mu_2/\mu_1) \quad (\text{A2})$$

To implement the Kalman observer, the model in (A1) is rewritten in a discrete time, linear, time invariant state space format of the following form (\mathbf{u}_k are the deterministic reactor feed streams, C_i and C_m ; $w_k \sim N(0, q)$ is the stochastic component or uncertainty in the feed stream C_i ; y_k is the conversion measurement at discrete time point k , where measurements are performed every Δt seconds (the time between successive discrete observations); $v_k \sim N(0, r)$ is the analysis error).^{3,4}

$$\mathbf{x}_k = \mathbf{A}\mathbf{x}_{k-1} + \mathbf{B}_1\mathbf{u}_{k-1} + \mathbf{b}_2w_{k-1} \quad y_k = \mathbf{c}'\mathbf{x}_k + v_k \quad (\text{A3})$$

In (A3), the system matrix \mathbf{A} contains all the dynamics and kinetics from model A1, and the input distribution \mathbf{B}_1 and \mathbf{b}_2 are the connection between deterministic and stochastic process input and the system, respectively. Measurement vector \mathbf{c} selects the sampled process variable y_k from state vector \mathbf{x}_k .

The mass balances for C_i , C_m , and λ_0 can be separated from the last five equations in (A1). This separation is possible because there is no backward coupling between the last five equations and the first three. Reduced state vector \mathbf{x}_k for the dynamic observer holds values for these first three process variables on equidistant grid points over the reactor tube length. The values for the five remaining mass balances on every grid point in the state vector \mathbf{x}_k are determined numerically using the estimated state vector elements as boundary conditions. The *process analyzer dynamics* as formulated in the Theory section can be incorporated in the system by appropriately augmenting matrix \mathbf{A} and state vector \mathbf{x}_k .³

The implementation of the Kalman state observer consists of two parts: (i) the state estimation time update (known as a priori estimate or “−”, the state transition between two discrete

measurements)

$$\hat{\mathbf{x}}_k^- = \mathbf{A}\hat{\mathbf{x}}_{k-1}^+ + \mathbf{B}_1\mathbf{u}_{k-1} \quad \mathbf{P}_k^- = \mathbf{A}\mathbf{P}_{k-1}^- \mathbf{A}' + \mathbf{Q}^{\Delta t} \quad (\text{A4})$$

(ii) the state estimate measurement update (known as a posteriori estimate or “+”, correcting the state estimate when measurement y_k becomes available)

$$\begin{aligned} \hat{\mathbf{x}}_k^+ &= \hat{\mathbf{x}}_k^- + \mathbf{k}_k(y_k - \mathbf{c}'\hat{\mathbf{x}}_k^-) & \mathbf{P}_k^+ &= (\mathbf{I} - \mathbf{k}_k\mathbf{c}')\mathbf{P}_k^- \\ \mathbf{k}_k &= \mathbf{P}_k^- \mathbf{c}(\mathbf{c}'\mathbf{P}_k^- \mathbf{c} + r)^{-1} \end{aligned} \quad (\text{A5})$$

Where \mathbf{k}_k is the observer gain, \mathbf{P}_k is the theoretical estimation error covariance matrix, and $\mathbf{Q}^{\Delta t}$ is the uncertainty distribution covariance matrix. The matrix $\mathbf{Q}^{\Delta t}$ holds the contribution of the process disturbance w_k on the overall state estimation error, buildup over the time period Δt between two process measurements (see also sample frequency $1/T_i$ in Theory section). For a stable system matrix \mathbf{A} , there is an upper bound on the system uncertainty covariance matrix by $\mathbf{Q}^{\Delta t}$ for $\Delta t \rightarrow \infty$. This \mathbf{Q}^∞ corresponds to the maximum uncertainty in knowledge about the state of the process for the situation where no in-process measurements are implemented.

For linear time invariant systems, the theoretical estimation error \mathbf{P}_k can be calculated a priori by solving the associated equations in (A4) and (A5). When an analyzer/observer combination is used to make an estimate, part of the uncertainty about the process state will be removed. Estimation error covariance matrix \mathbf{P}_k then gives the process state uncertainty that remains. A suitable norm of the estimation covariance matrix \mathbf{P}_k can thus guide the selection of optimal process analyzer and type and position. The matrix trace norm—sum of all variances on the diagonal—is an appropriate choice here.

Received for review March 6, 2002. Accepted March 22, 2002.

AC020148W